

An Approach to Evaluate the Region of Attraction of Satellites controlled by SDRE

ALESSANDRO GERLINGER ROMERO
Space Mechanics and Control Division
National Institute of Space Research
Astronautas Avenue, 1758 - São José dos Campos
BRAZIL

LUIZ CARLOS GADELHA DE SOUZA
Engineering Center
Federal University of ABC
dos Estados Avenue - São Bernardo do Campo
BRAZIL

Abstract: The control of a satellite can be designed with success by linear control theory if the satellite has slow angular motions. However, for fast maneuvers, the linearized models are not able to represent the effects of the nonlinear terms. One candidate technique for the design of the satellite's control under fast maneuvers is the State-Dependent Riccati Equation (SDRE). SDRE provides an effective algorithm for synthesizing nonlinear feedback control by allowing nonlinearities. Nonetheless, much criticism has been leveled against the SDRE because it does not provide assurance of global asymptotic stability. Additionally, there are situations in which global asymptotic stability cannot be achieved (e.g., systems with multiple equilibrium points). Therefore, especially in aerospace, estimating the region of attraction (ROA) is fundamental. The Brazilian National Institute for Space Research (INPE, in Portuguese) was demanded by the Brazilian government to build remote-sensing satellites, such as the Amazonia-1 mission. In such missions, the satellite must be stabilized in three axes so that the optical payload can point to the desired target. In this paper, we share an approach to evaluate the ROAs of Amazonia-1 controlled by LQR (the linear counterpart of SDRE) and SDRE. The initial results showed SDRE has a larger ROA than LQR.

Key-Words: Nonlinear, control, SDRE, LQR, Region of Attraction.

Received: June 22, 2021. Revised: March 17, 2022. Accepted: April 19, 2022. Published: May 7, 2022.

1 Introduction

The design of a satellite attitude and orbit control subsystem (AOCS) that involves plant uncertainties, large-angle maneuvers, and fast attitude control following a stringent pointing, requires nonlinear control techniques in order to satisfy performance and robustness requirements. An example is a typical mission of the Brazilian National Institute for Space Research (INPE), in which the AOCS must stabilize a satellite in three axes so that the optical payload can point to the desired target with few arcsecs of pointing accuracy.

One candidate technique for a nonlinear AOCS control law is the State-Dependent Riccati Equation (SDRE). SDRE is based on the arrangement of the system model in a form known as state-dependent coefficient (SDC) matrices. Accordingly, a suboptimal control law is carried out by a real-time solution of an algebraic Riccati equation (ARE) using the SDC matrices by means of a numerical algorithm.

SDRE was originally proposed by [1] and then explored in detail by [2]. A good survey of the SDRE

technique can be found in [3] and its systematic application to deal with a nonlinear plant in [4]. The SDRE technique was applied by [5, 6, 7, 8, 9] for controlling a nonlinear system similar to the six-degree of freedom satellite model considered in this paper.

The application of the SDRE technique, and, consequently, the ARE problem that arises, have already been studied in the available literature, e.g., [10] investigated the approaches for the ARE solving as well as the resource requirements for such online solving. Recently, [6] proposed the usage of differential algebra to reduce the resource requirements for the real-time implementation of SDRE controllers. In fact, the intensive resource requirements for the online ARE solving is the major drawback of SDRE. Nonetheless, the SDRE has three major advantages: (a) simplicity, (b) numerical tractability, and (c) flexibility for the designer, being comparable to the flexibility in the LQR [6].

The origin of an SDRE controlled system is a locally asymptotically stable equilibrium point [2]. Furthermore, the knowledge of its region of attraction is

fundamental due to the local stability even more in the presence of nonlinearities.

Indeed, much criticism has been leveled against the SDRE technique since it does not provide assurance of global asymptotic stability. However, empirical experience shows that in many cases the region of attraction (ROA) may be as large as the domain of interest [3]. Moreover, there are situations in which global asymptotic stability cannot be achieved (for example, systems with multiple equilibrium points). Therefore, especially in aerospace, estimating the region of attraction is fundamental [3].

Obtaining a good estimate of such a ROA, especially of a higher-order system, is a challenging task in itself. In fact, [11] states that analytical ROA for nonlinear systems with dimensions greater than two is usually unavailable. Such a task becomes even more difficult since the closed-loop matrix of SDRE is usually not available in the closed form [12].

The well-known Lyapunov approaches to estimate the region of attraction cannot be used for SDRE since the closed-loop system equations are usually not known explicitly. [12, 13] proposed procedures to reduce the effort of ROA's computation focusing on the maximum and the minimum values of feedback gains over a chosen region of the statespace. The other alternative is to make time-domain simulations of the closed-loop system, which is cumbersome and costly [12, 13].

In this paper, we share an approach to evaluate the ROA of Amazonia-1 controlled by LQR (linear-quadratic regulator, the linear counterpart of SDRE) and SDRE. The initial results showed SDRE has a larger ROA than LQR in the presence of nonlinearities. Recall LQR guarantees global stability for linear systems (afterward, the linearization process), nevertheless, such a property is lost when nonlinearities are accounted for.

In Section 2, the problem description is presented. In Section 3, the satellite physical modeling is reviewed. In Section 4, we explore the state-space model, the controllers, and the approach for the ROAs. In Section 5, we share simulation results. Finally, the conclusions are shared in Section 6.

2 Problem Description

The SDRE technique entails factorization (that is, parametrization) of the nonlinear dynamics into the state vector and the product of a matrix-valued function that depends on the state itself. In doing so, SDRE brings the nonlinear system to a (nonunique) linear structure having SDC matrices given by Eq. (1).

$$\begin{aligned}\dot{\vec{x}} &= A(\vec{x})\vec{x} + B(\vec{x})\vec{u} \\ \vec{y} &= C\vec{x}\end{aligned}\quad (1)$$

where $\vec{x} \in \mathbb{R}^n$ is the state vector and $\vec{u} \in \mathbb{R}^m$ is the control vector. Notice that the SDC form has the same structure as a linear system, but with the system matrices, A and B , being functions of the state vector. The nonuniqueness of the SDC matrices creates extra degrees of freedom, which can be used to enhance controller performance, however, it poses challenges since not all SDC matrices fulfill the SDRE requirements, e.g., the pair (A,B) must be pointwise stabilizable.

The system model in Eq. (1) is subject of the cost functional described in Eq. (2).

$$J(\vec{x}_0, \vec{u}) = \frac{1}{2} \int_0^\infty (\vec{x}^T Q(\vec{x})\vec{x} + \vec{u}^T R(\vec{x})\vec{u}) dt \quad (2)$$

where $Q(\vec{x}) \in \mathbb{R}^{n \times n}$ and $R(\vec{x}) \in \mathbb{R}^{m \times m}$ are the state-dependent weighting matrices. In order to ensure local stability, $Q(\vec{x})$ is required to be positive semi-definite for all \vec{x} and $R(\vec{x})$ is required to be positive for all \vec{x} [10].

The SDRE controller linearizes the plant about the current operating point and creates constant statespace matrices so that the LQR can be used. This process is repeated in all samplings steps, resulting in a pointwise linear model from a non-linear model, so that an ARE is solved and a control law is computed also in each step. Therefore, according to LQR theory and Eq. (1) and (2), the state-feedback control law in each sampling step is $\vec{u} = -K(\vec{x})\vec{x}$ and the state-dependent gain $K(\vec{x})$ is obtained by Eq. (3) [4].

$$K(\vec{x}) = R^{-1}(\vec{x})B^T(\vec{x})P(\vec{x}) \quad (3)$$

where $P(\vec{x})$ is the unique, symmetric, positive-definite solution of the algebraic state-dependent Riccati equation (SDRE) given by Eq. (4) [4].

$$\begin{aligned}P(\vec{x})A(\vec{x}) + A^T(\vec{x})P(\vec{x}) \\ - P(\vec{x})B(\vec{x})R^{-1}(\vec{x})B^T(\vec{x})P(\vec{x}) \\ + Q(\vec{x}) = 0\end{aligned}\quad (4)$$

Considering that Eq. (4) is solved in each sampling step, it is reduced to an ARE. Finally, the conditions for the application of the SDRE technique in a given system model are [4]:

1. $A(\vec{x}) \in C^1(\mathbb{R}^w)$
2. $B(\vec{x}), C(\vec{x}), Q(\vec{x}), R(\vec{x}) \in C^0(\mathbb{R}^w)$
3. $Q(\vec{x})$ is positive semi-definite and $R(\vec{x})$ is positive definite
4. $A(\vec{x})x \implies A(0)0 = 0$, i.e., the origin is an equilibrium point

5. $pair(A, B)$ is pointwise stabilizable (a sufficient test for stabilizability is to check the rank of controllability matrix)
6. $pair(A, Q^{\frac{1}{2}})$ is pointwise detectable (a sufficient test for detectability is to check the rank of observability matrix)

2.1 Region of Attraction

One is frequently interested in the region of attraction (ROA; also called domain of attraction or basin of attraction), i.e., the region of the statespace in which the initial conditions of the trajectories lie in order to attain stable behavior [14].

Equilibrium points, if exist, must lie in the regions of attraction, indeed, a state $x_e \in \mathcal{R}^n$ is an equilibrium point of a nonlinear dynamical system $\dot{x} = f(x)$ if $x_0 = x_e \implies x(t) = x_e, \forall t > 0$ so $f(x_e) = 0$. A nonlinear system can have an infinite number of equilibrium points, and, each one can be stable or unstable. Additionally, to investigate the stability of a particular equilibrium point x_0 it is convenient to transform the equilibrium point to the origin $x^* = 0$ through the transformation $x^* = x - x_0$ [14].

Such equilibrium points, if exist, lie in the regions of attraction, which are defined by their attractors. An attractor is a subset $A \in \mathcal{R}^n$ of the statespace characterized by the following three conditions: (i) $a \in A \implies f(a, t) \in A, \forall t > 0$; (ii) there exists a vicinity of A (region of attraction) which consists of all trajectories that enter A for $t \rightarrow \infty$; and, (iii) there is no proper (non-empty) subset of A having the first two properties. The attractors can be classified in: (I) Fixed point - the final state that a dynamic system evolves towards corresponds to an attracting fixed point, i.e., stable equilibrium point; (II) Limit cycle - a periodic orbit; (III) Quasiperiodic - it exhibits irregular periodicity; (IV) Strange attractor - when such sets cannot be easily described.

Regarding the fixed point attractor, it can be defined by the following equation [15].

$$A = \{x_0 \in \mathcal{R}^n : \lim_{t \rightarrow +\infty} x(t, x_0) = 0\} \quad (5)$$

It is important for practical reasons to have information about the size and/or the shape of A . Indeed, the stability properties could be of scarce utility if the region of attraction is very small, or if the equilibrium point is very close to its boundary. There is a wide literature about theoretical methods for the determination of A , and about numerical methods for its approximate estimation [12, 15, 13].

3 Satellite Physical Modeling

Focusing on a typical mission developed by INPE, the AOCS must stabilize a satellite in three axes so that

the optical payload can point to the desired target. The next subsections explore the kinematics and the rotational dynamics of the satellite attitude available in the simulator.

3.1 Kinematics

Given the ECI reference frame (\mathfrak{F}_i) and the frame defined in the satellite with origin in its centre of mass (the body-fixed frame, \mathfrak{F}_b), then a rotation $R \in SO(3)$ ($SO(3)$ is the set of all attitudes of a rigid body described by 3×3 orthogonal matrices whose determinant is one) represented by a unit quaternion $Q = [q_1 \ q_2 \ q_3 \ | \ q_4]^T$ can define the attitude of the satellite.

Defining the angular velocity $\vec{\omega} = [\omega_1 \ \omega_2 \ \omega_3]^T$ of \mathfrak{F}_b with respect to \mathfrak{F}_i measured in the \mathfrak{F}_b , the kinematics can be described by Eq. (6) [16].

$$\dot{Q} = \frac{1}{2} \Omega(\vec{\omega}) Q \quad (6)$$

$$\Omega(\vec{\omega}) \triangleq \begin{bmatrix} 0 & \omega_3 & -\omega_2 & \omega_1 \\ -\omega_3 & 0 & \omega_1 & \omega_2 \\ \omega_2 & -\omega_1 & 0 & \omega_3 \\ -\omega_1 & -\omega_2 & -\omega_3 & 0 \end{bmatrix}$$

where the unit quaternion Q satisfies the following identity:

$$q_1^2 + q_2^2 + q_3^2 + q_4^2 = 1 \quad (7)$$

Eq. (6) allows the prediction of the satellite's attitude if it is available the initial attitude and the history of the change in the angular velocity ($\dot{Q} = F(\omega, t)$). Another possible derivation of the Eq. (6) is using the vector g (Gibbs vector or Rodrigues parameter) as $Q = [g^T | q_4]$.

$$\dot{Q} = -\frac{1}{2} \begin{bmatrix} \omega^\times \\ \omega^T \end{bmatrix} \begin{bmatrix} q_1 \\ q_2 \\ q_3 \end{bmatrix} + \frac{1}{2} q_4 \begin{bmatrix} 1_{3 \times 3} \\ 0 \end{bmatrix} \vec{\omega} \quad (8)$$

where ω^\times is the cross-product skew-symmetric matrix of $\vec{\omega}$ and 1 is the identity matrix. Note the Gibbs vector is geometrically singular since it is not defined for 180° of rotation [17], nonetheless, the Eq. (8) is global.

3.2 Rotational Dynamics

The satellite has a set of 3 reaction wheels, each one aligned with its principal axes of inertia, moreover, such type of actuator, momentum exchange actuators, does not change the angular momentum of the satellite. Consequently, it is mandatory to model their influence in the satellite, in particular, the angular mo-

mentum of the satellite is defined by Eq. (9).

$$\vec{h} = (\mathbf{I} - \sum_{n=1}^3 I_{n,s} a_n a_n^T) \vec{\omega} + \sum_{n=1}^3 h_{w,n} \vec{a}_n \quad (9)$$

where \mathbf{I} is the inertia tensor, $I_{n,s}$ is the inertia moment of the n reaction wheel in its symmetry axis \vec{a}_n , $h_{w,n}$ is the angular momentum of the n reaction wheel about its centre of mass ($h_{w,n} = I_{n,s} a_n^T \omega + I_{n,s} \omega_n$) and ω_n is the angular velocity of the n reaction wheel.

One can define $I_b = \mathbf{I} - \sum_{n=1}^3 I_{n,s} a_n a_n^T$. Using I_b , the motion of the satellite is described by Eq. (10).

$$I_b \dot{\omega}^b = g_{cm} - \omega^\times (I_b \omega + \sum_{n=1}^3 h_{w,n} a_n) - \sum_{n=1}^3 g_n a_n \quad (10)$$

where g_{cm} is the net external torque and g_n are the torques generated by the reactions wheels ($h_{w,n} = g_n$).

4 Controller Design and ROA

Two dynamics states must be controlled: (1) the attitude (modeled as unit quaternions Q by Equation (6) or Equation (8)) and (2) its stability (\dot{Q} , in other words, the angular velocity ω of the satellite by Equation (10)). The following subsections explore the state-space modeling and the synthesis of controllers.

4.1 Linear Control based on LQR

Equation (6) and Equation (7) can be used to linearize the system around a stationary point ($\omega = 0$ and $Q = [0 \ 0 \ 0 \ -1]^T$, assuming there is no net external torque, $g_{cm} = 0$), which leads to Equation (11).

$$\begin{bmatrix} x_1 \\ x_2 \end{bmatrix} = \begin{bmatrix} Q \\ \omega \end{bmatrix} \quad (11)$$

$$\begin{bmatrix} \dot{x}_1 \\ \dot{x}_2 \end{bmatrix} = \begin{bmatrix} 0 & -\frac{1}{2} I_{3 \times 3} \\ 0 & 0 \\ 0 & 0 \end{bmatrix} \begin{bmatrix} x_1 \\ x_2 \end{bmatrix} + \begin{bmatrix} 0 \\ 0 \\ -I_b^{-1} \end{bmatrix} [u_1]$$

$$[y] = I \begin{bmatrix} x_1 \\ x_2 \end{bmatrix}$$

Equation (11) defines the constant matrixes A, B and C for a linear state-space representation of Amazonia-1 (see Table 1) around the stationary point. However, the constant matrixes A and B are not stabilizable since the controllability matrix of the pair(A,B) has no full rank. Indeed, [18] showed that this linearized model with all quaternion components was not stabilizable, meaning that LQR is not applicable.

Equation (7) defines a direct method to find q_4 , therefore, one option is to model the state of the system without such component of the quaternion [18], which leads to the following equation:

$$\begin{bmatrix} x_3 \\ x_2 \end{bmatrix} = \begin{bmatrix} q_1 \\ q_2 \\ q_3 \\ \omega \end{bmatrix} \quad (12)$$

$$\begin{bmatrix} \dot{x}_3 \\ \dot{x}_2 \end{bmatrix} = \begin{bmatrix} 0 & -\frac{1}{2} I_{3 \times 3} \\ 0 & 0 \end{bmatrix} \begin{bmatrix} x_3 \\ x_2 \end{bmatrix} + \begin{bmatrix} 0 \\ -I_b^{-1} \end{bmatrix} [u_1]$$

$$[y] = I \begin{bmatrix} x_3 \\ x_2 \end{bmatrix}$$

Equation (12) defines the constant matrixes A, B and C for an alternative linear state-space representation of Amazonia-1 (see Table 1) around the stationary point. In such the statespace, constant matrixes A and B are stabilizable.

4.2 Nonlinear Control based on SDRE

Assuming that there are no net external torques ($g_{cm} = 0$), the statespace model can be defined using Eq. (6) (Ω) and (10), however, the SDC matrixes do not fulfill the SDRE requirements, in particular, the pair (A,B) is not pointwise stabilizable.

An option for the definition of the SDC matrixes is to use Eq. (8), which leads to Eq. (13).

$$\begin{bmatrix} \dot{x}_1 \\ \dot{x}_2 \end{bmatrix} = \begin{bmatrix} -\frac{1}{2} \begin{bmatrix} \omega^\times \\ \omega^T \end{bmatrix} & 0 & \begin{bmatrix} \frac{1}{2} q_4 I_{3 \times 3} \\ 0 \end{bmatrix} \\ 0 & 0 & -I_b^{-1} \omega^\times I_b + I_b^{-1} (\sum_{n=1}^3 h_{w,n} a_n)^\times \end{bmatrix} \begin{bmatrix} x_0 \\ x_2 \end{bmatrix} + \begin{bmatrix} 0 \\ -I_b^{-1} \end{bmatrix} [u_1] \quad (13)$$

$$[y] = I \begin{bmatrix} x_0 \\ x_2 \end{bmatrix}$$

Eq. (13) has been shown to satisfy SDRE conditions described in Section 2.

Equation (13) has been shown to satisfy SDRE conditions in the majority of statespace with exception of the region on which the angular velocity is close to 0 (the pair(A,B) loses rank in such region). In practical problems, regarding such a region, one approach is to switch to another SDC parametrization [11] or to resort to LQR. Note such the known limitation of this particular parametrization of SDRE imposes laxity.

Table 1: Satellite characteristics, initial conditions and references.

Name	Value
Satellite Characteristics	
inertia tensor ($kg.m^2$), I	$\begin{bmatrix} 310.0 & 1.11 & 1.01 \\ 1.11 & 360.0 & -0.35 \\ 1.01 & -0.35 & 530.7 \end{bmatrix}$
Actuators Characteristics - Reaction Wheels	
inertia tensor of 3 reaction wheels ($kg.m^2$), $\sum_{n=1}^3 I_{n,s} a_n a_n^T$	$diag(0.01911, 0.01911, 0.01911)$
maximum torque ($N.m$)	0.075
maximum angular velocity (RPM)	6000
Initial conditions	
attitude ($degrees$, XYZ)	$[0 \ 0 \ 180]^T$
angular velocity ($radians/second$, XYZ)	$[0 \ 0 \ 0.024]^T$
References for the controller	
solar vector in the body (XYZ)	$[1 \ 0 \ 0]^T$
angular velocity ($radians/second$, XYZ)	$[0 \ 0 \ 0]^T$

4.3 Region of Attraction

Firstly, the control laws, independent of the applied technique being linear or nonlinear, are modeled and too many time-domains simulations are available for their analysis. Furthermore, in the presence of nonlinearities even the techniques that guarantee global asymptotically stability can lose such property. Therefore, the main task is to assess the presence of a fixed point attractor as well as its size and shape.

Nonetheless, it is somewhat difficult to depict the ROA for statespace systems with dimensions higher than three. Facing such difficulty, [11] chose to list the domain of interest and to plot a small subset of simulations. Such an approach offers restricted support for the comparison of different ROAs.

Inspired by the works of Henri Poincaré, in particular, Poincaré maps [19] which defines a lower-dimensional subspace for qualitative analysis. The present paper applied two euclidean norms, namely L2-norm of Euler angles and L2-norm of angular velocities, to define a two-dimensional space for qualitative and quantitative analysis. In such a way that the area of the ROA (dimensionless quantity) can be analytically computed and compared; and, the plot of the ROA can allow straightforward qualitative analysis.

Besides, the definition of the fixed point attractor presented in Equation (5) is restricted by the definition of an explicit final time t_f and a numerical error ϵ , according to the following equation:

$$A = \{x_0 \in \mathcal{R}^n : \lim_{t \rightarrow t_f} \|x(t, x_0)\|_2 < \epsilon\} \quad (14)$$

Equipped with (A) the two-dimensional space for qualitative analysis of the original up to seven-dimensional statespace, and (B) Equation (14), simple

polygons (they do not intersect themselves and have no holes) of ROAs are defined in the two-dimensional space for the initial conditions x_0 . The area of such polygons is the main measure for the quantitative comparison of different control laws.

Taking into account the limitations of the control laws previously stated in Subsection 4.2, the definition of the fixed point attractor presented in Equation (14) is once restricted by the selection of sole angular velocities (x_2 in Equation (11), Equation (12), and Equation (13)), ω -stability in [16], according to the following equation:

$$A = \{x_0 \in \mathcal{R}^n : \lim_{t \rightarrow t_f} \|x_2(t, x_0)\|_2 < \epsilon\} \quad (15)$$

Focusing on the area of ROAs A , one defines a Monte Carlo perturbation model for a given initial conditions, performs the time-domain simulation until the predefined t_f , and, finally, computes the measure.

5 Simulation Results

The results were computed using the satellite (modeled as a nonlinear system) and the control laws (LQR, and SDRE) with nonlinearities in the reaction wheels, i.e., maximum torque and maximum angular velocity. Furthermore, such the results were obtained running a full Monte Carlo perturbation model described as follows.

Regarding initial attitudes defined by 3-2-1 Euler angles (Z-Y-X, nonclassical Euler angles), it is well-known that representing Y beyond ± 90 degrees (that means ± 180 degrees) would give two Euler angles solution for every rotation, so Y is limited to

± 90 degrees. X and Z are limited to ± 180 degrees. Therefore, independent distributions are applied for each Euler angle respecting the limits previously discussed in order to define the initial attitudes (3-2-1, Z-Y-X, nonclassical Euler angles, which are converted in quaternions) in a given Monte Carlo perturbation model.

Regarding initial angular velocities, they are defined by independent distributions based on the maximum angular velocity of the satellite that is controllable by the reaction wheels. Using Section 3.2 and Table 1, the maximum angular momentum of the set of reactions wheels was computed ($h_{w_{max}} = \vec{I}_w \cdot \vec{\omega}_{w_{max}}$) and then the corresponding maximum angular velocity of the satellite was found solving a matrix equation ($h_{w_{max}} = \vec{I} \cdot \vec{\omega}_{max}$). The result in radians per second was $\omega_{max} = \{0.0385, 0.0332, 0.0225\}$, the norm (L2) was 0.0556, and the infinity norm was 0.0385, which is the value used as parameter in Table 2.

In summary, the approach for the evaluation of the region of attraction can be summarized as:

- Compute initial conditions for the Monte Carlo perturbation model

Using independent distributions, compute the 3-2-1 Euler angles (Z-Y-X, nonclassical Euler angles) in the range ($\pm 180, \pm 90, \pm 180$)

Using independent distributions, compute the angular velocities based on the maximum angular velocity of satellite that is controllable by the reaction wheels

- Perform the time-domain simulation until the predefined t_f
- Compute ROAs

The results are based on the satellite Amazonia-1, which is characterized by Table 1, furthermore, the simulations were conducted with the full Monte Carlo perturbation model tuned with the parameters shared in Table 2.

The initial conditions uniformly distributed computed using such parameters by the Monte Carlo perturbation model are depicted using a two-dimensional space, in which the norm of Euler angles is along the X-axis and the norm of angular velocities is along the Y-axis for each initial condition. This space has its bounds constrained by the norm of Euler Angles ranging from 0 to 270 degrees and the norm of angular velocities ranging from 0 to 0.066 radians per second, following the parameters presented in Table 2. However, as there is no mechanism to desaturate the reactions wheels, the limit expected for the norm of the angular velocities of the initial conditions inside any

ROA is the previously shared 0.0556 radians per second (in the presence of the nonlinearities). The same two-dimensional space is used to depict ROAs.

Figure 1 shows the initial conditions uniformly distributed by such a Monte Carlo perturbation model execution (400 simulations, two different control laws for each initial condition).

Taking into account the applied nonlinearities in the reaction wheels (maximum torque, and maximum angular velocity), for any step of a given maneuver the actual control torque generated by the reaction wheels could be smaller than the computed control. Indeed, with such nonlinearities, the actual control was smaller than the computed control in the simulations as shown in Figure 2. Note points are close to the X-axis in the sense that actual control was much smaller than the bisectrix (where actual equals computed control).

The result of such a “lack of control” is depicted in Figure 3 that shows the ROA of LQR (in blue, legend ProportionalLinearQuaternionPartialLQRController), and SDRE (in red, legend ProportionalNonLinearQuaternionSDREController_GIBBS).

The number of samples that converged by Equation (15) is less than the initial conditions, therefore, the global asymptotic stability property is not present in LQR or SDRE. Nonetheless, the ROA of the SDRE is larger since more initial conditions converged for t_f . Moreover, both control laws are able to control the whole range of Euler angles, consequently, the angular velocities are the critical aspects to be constrained in the initial conditions. Such the fact corroborates ω -stability [16] as the major concern in accordance with Equation (15). Furthermore, it confirms the common sense the controlling of angular velocities is constrained by nonlinearities in the actuators leading to saturation.

6 Conclusion

As the results are based on analysis through simulations, they are neither valid for general cases nor for scenarios out of the range of the Monte Carlo perturbation models due to the underlining nonlinear dynamics.

Although the results provide empirical evidence that SDRE has a larger ROA than LQR in the case of Amazonia-1, the major contribution of the paper is the approach for the evaluation of the ROAs since such the approach provides a tractable numerical algorithm to compare control techniques. Moreover, confidence turns to be a matter of computational power.

References:

- [1] J. D. Pearson, “Approximation methods in optimal control i. sub-optimal control,” *Journal of*

Table 2: Monte Carlo perturbation model parameters.

Name	Value
3-2-1 Euler angles (degrees)	$Z : U(-180, 180)$ $Y : U(-90, 90)$ $X : U(-180, 180)$
angular velocities (rad/s)	$X : U(-0.0385, 0.0385)$ $Y : U(-0.0385, 0.0385)$ $Z : U(-0.0385, 0.0385)$
Q	I
R	I
ϵ (rad/s)	0.0001
samples	200
t_f (seconds)	3600
fixed step size (seconds)	0.05

Electronics and Control, vol. 13, no. 5, pp. 453–469, 1962.

- [2] J. R. Cloutier, C. N. D’Souza, and C. P. Mracek, “Nonlinear regulation and nonlinear H-infinity control via the state-dependent Riccati equation technique.,” *Conference on Nonlinear Problems in Aviation*, 1996.
- [3] T. Çimen, “State-Dependent Riccati Equation (SDRE) control: a survey,” *IFAC Proceedings Volumes (IFAC-PapersOnline)*, vol. 17, no. 1 pt. 1, pp. 3761–3775, 2008.
- [4] T. Çimen, “Systematic and effective design of nonlinear feedback controllers via the state-dependent Riccati equation (SDRE) method,” *Annual Reviews in Control*, vol. 34, no. 1, pp. 32–51, 2010.
- [5] R. G. Gonzales and L. C. G. d. Souza, “Application of the sdre method to design a attitude control system simulator,” *Advances in the Astronautical Sciences*, vol. 134, no. Part 1-3, pp. 2251–2258, 2009.
- [6] G. DiMauro, M. Schlotterer, S. Theil, and M. Lavagna, “Nonlinear control for proximity operations based on differential algebra,” *Journal of Guidance, Control, and Dynamics*, vol. 38, pp. 2173–2187, apr 2015.
- [7] A. G. Romero, L. C. G. Souza, and R. A. Chagas, *Application of the SDRE Technique in the Satellite Attitude and Orbit Control System with Nonlinear Dynamics*. 2018.
- [8] A. G. Romero and L. C. G. Souza, “Application of the sdre technique based on java in a cubesat attitude and orbit control subsystem,” in *Proceedings...*, IAA Latin American CubeSat, December 2018.
- [9] A. G. Romero, *Application of the SDRE technique in the satellite attitude and orbit control system with nonlinear dynamics*. PhD thesis, Instituto Nacional de Pesquisas Espaciais (INPE), São José dos Campos, 2021-12-07 2022.
- [10] P. K. Menon, T. Lam, L. S. Crawford, and V. H. Cheng, “Real-time computational methods for SDRE nonlinear control of missiles,” *Proceedings of the American Control Conference*, vol. 1, pp. 232–237, 2002.
- [11] J. Yao, Q. Hu, and J. Zheng, “Nonlinear optimal attitude control of spacecraft using novel state-dependent coefficient parameterizations,” *Aerospace Science and Technology*, vol. 112, p. 106586, 2021.
- [12] E. Erdem and A. Alleyne, “Estimation of stability regions of sdre controlled systems using vector norms,” in *Proceedings...*, vol. 1, pp. 80–85 vol.1, American Control Conference, 2002.
- [13] A. Bracci, M. Innocenti, and L. Pollini, “Estimation of the region of attraction for state-dependent riccati equation controllers,” *Journal of Guidance, Control, and Dynamics*, vol. 29, no. 6, pp. 1427–1430, 2006.
- [14] P. C. Parks and V. Hahn, *Stability Theory*. New York: Prentice-Hall, 1992.
- [15] L. Bacciotti, A.; Rosier, *Liapunov functions and stability in control theory*. Berlin, Germany: Springer, 2 ed., 2005.
- [16] P. C. Hughes, *Spacecraft attitude dynamics*. New York, 1986.
- [17] P. W. Fortescue and G. G. Swinerd, “Attitude control,” *Spacecraft Systems Engineering*, pp. 289–326, 2011.

- [18] Y. Yang, “Analytic LQR design for spacecraft control system based on quaternion model,” *Journal of Aerospace Engineering*, vol. 25, no. 3, pp. 448–453, 2012.
- [19] H. Leipholz, *Stability theory: an introduction to the stability of dynamic systems and rigid bodies*. Academic Press, 1970.

Contribution of individual authors to the creation of a scientific article (ghostwriting policy)

Alessandro Gerlinger Romero carried out the modeling, the code developing, the simulation and the writing.

Luiz Carlos Gadelha de Souza oriented the first author and contributed in the writing.

Creative Commons Attribution License 4.0 (Attribution 4.0 International , CC BY 4.0)

This article is published under the terms of the Creative Commons Attribution License 4.0

https://creativecommons.org/licenses/by/4.0/deed.en_US

Figure 1: Initial conditions.

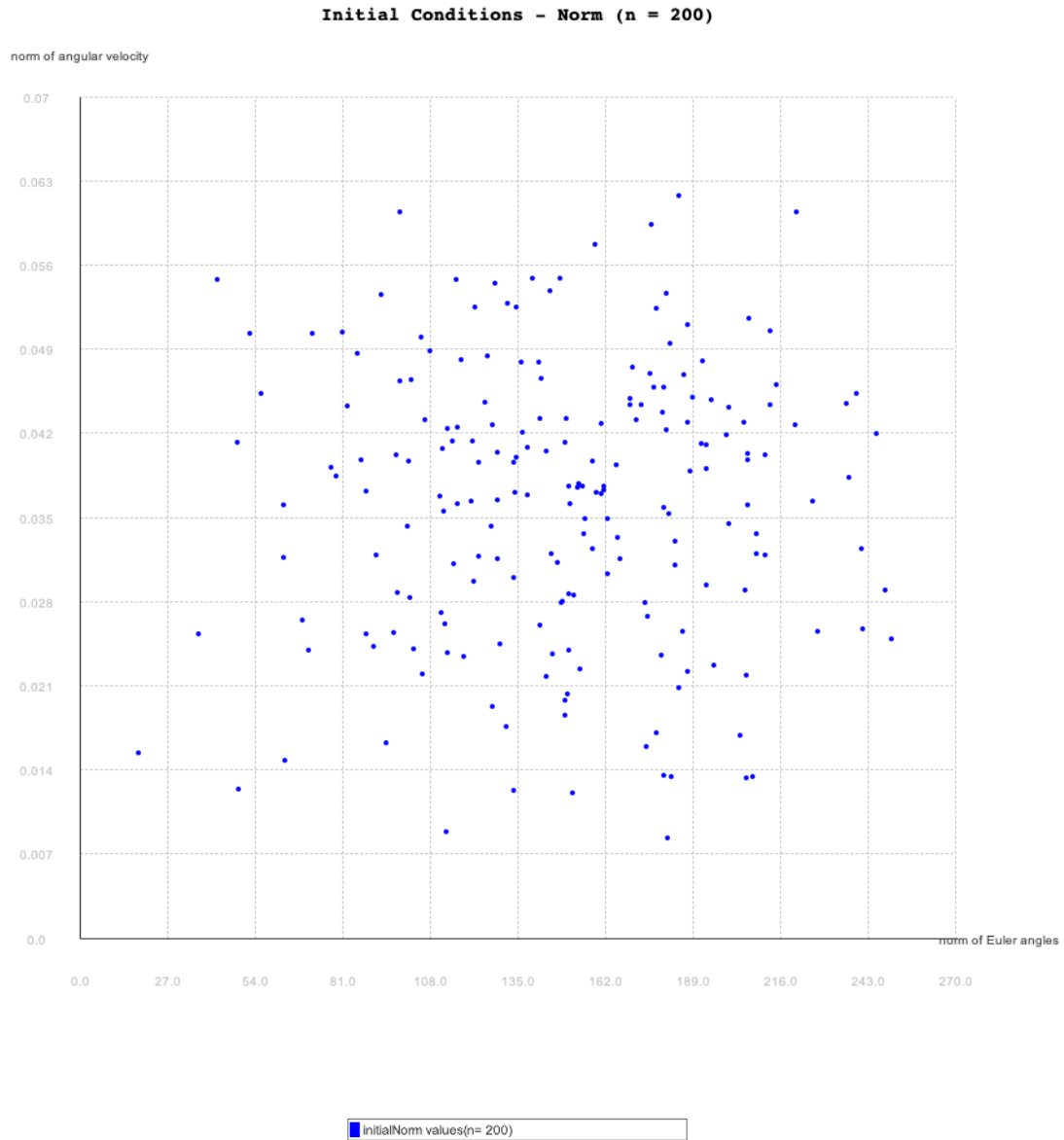


Figure 2: Actual versus computed control with nonlinearities in the reaction wheels.

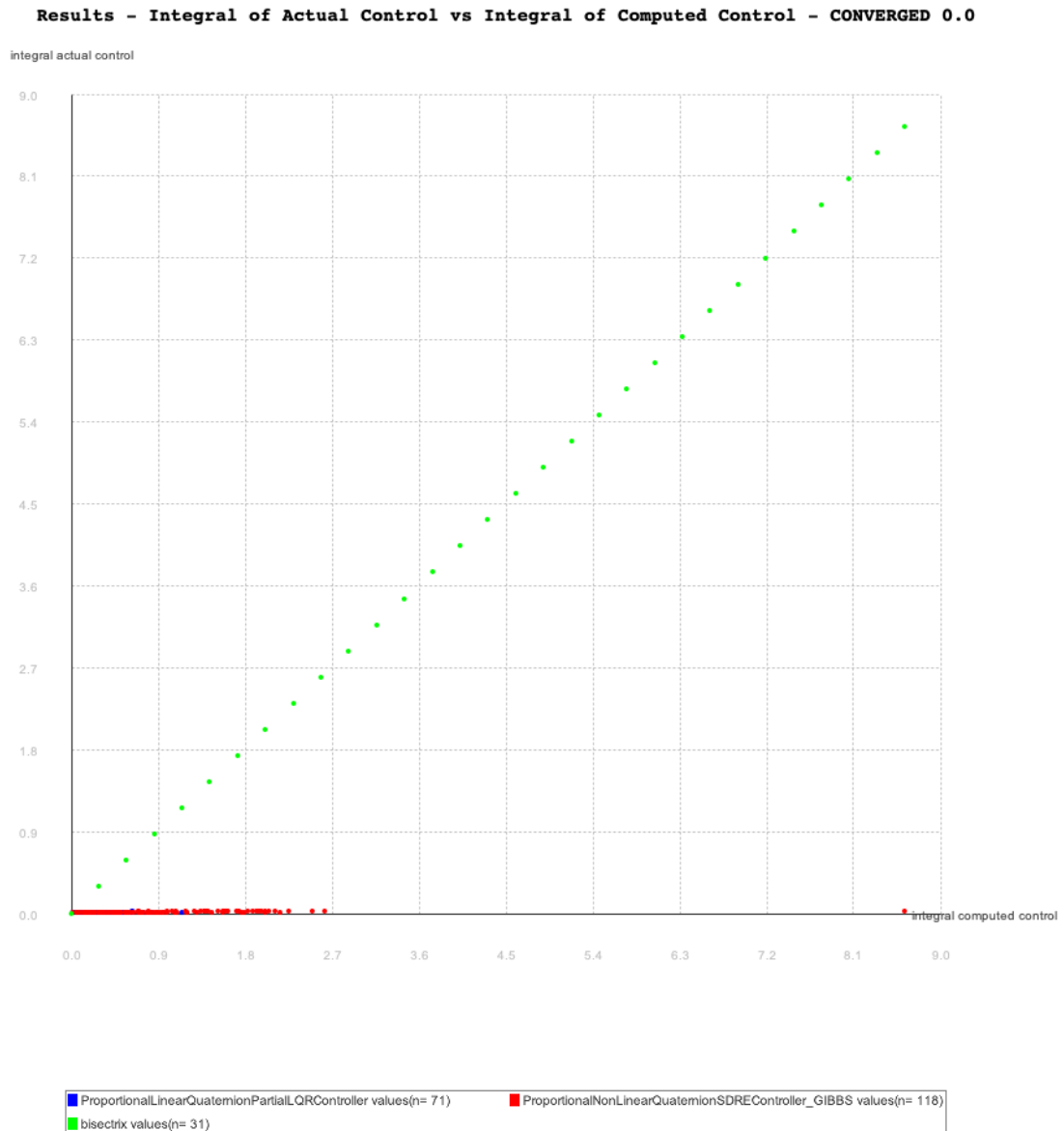


Figure 3: ROA with nonlinearities in the reactions wheels.

